One-Cell Analysis as a Technique for True Single-Cell Analysis of Organelles in Breast Tumor and Adjacent Normal Tissue to Profile Fatty Acid Composition of Triglyceride Species

Jason S. Hamilton and Guido F. Verbeck*

Department of Chemistry, University of North Texas, Denton, TX, USA

Abstract: Breast cancer develops in an adipose rich environment of normal adipocytes that are known to aid in tumor progression through an unknown method of lipid transfer from normal cells to tumor cells. Much research is built around lipid analysis of breast tumor and adjacent normal tissues to identify variations in the lipidome to gain an understanding of the role lipids play in progressing cancer. Ideally, single-cell analysis methods coupled to mass spectrometry that retain spatial information are best suited for this endeavor. However, many single-cell analysis methods are not capable of subcellular analysis of intact lipids while maintaining spatial information. One-Cell analysis is a true single-cell technique with the precision to extract single organelles from intact tissues while not interfering or disrupting adjacent cells. This method is used to extract and analyze single organelles from individual cells using nanomanipulation coupled to nanoelectrospray ionization mass spectrometry. Presented here is a demonstration of the analysis of single lipid bodies from two different sets of breast tumor and normal adjacent tissues to elucidate the fatty acid composition of triglycerides using One-Cell analysis coupled to tandem mass spectrometry. As a result, thirteen fatty acid species unique to the tumor tissues were identified, five in one set of tissues and eight in the other set.

Keywords: Single-cell, lipid body, tandem mass spectrometry, nanoelectrospray ionization, breast cancer.

1. INTRODUCTION

Breast cancer is the most commonly diagnosed site specific cancer and the second leading cancer-related cause of death in women [1]. Breast tumors reside in an environment favorable for progression. The microenvironment of breast tumors is comprised of vasculature, connective tissue, and adipocytes, which store triglycerides (TG) in an organelle called a lipid body. Adipocytes have been shown to play an important tumor-supporting role by providing tumor cells with a supply of fatty acids released through lipolysis during tumor progression [2-5]. Once these adipocytes begin to undergo lipolysis their lipid body releases its stores, and the cell undergoes a phenotypic change in which it decreases in size and takes on a fibroblast like nature at which time they are then termed cancer-associated adipocytes (CAA) [2]. Furthermore, Chajes et al. identified that the lipid composition of the breast adipose tissue is different from other adipose sites in the body [6]. Much research has been focused on changes in serum lipid profiles as an indicator of the onset of breast cancer [7-12], but this type of analysis does not provide information about the ever-changing tumor microenvironment that is needed to understand localized tumor progression.

Current tissue lipid analysis methods often involve chemical or mechanical lysis of multiple cells followed by multi-step extractions to isolate lipid species from other cellular components. These methods result in lipid profile data that is averaged across multiple cells or even cell types in the case of complex intact tissues. This averaging of data can overshadow cellular lipid heterogeneity as it pertains to normal cellular development [13] or diseased induced alterations, such as de novo lipogenesis that has been detected early in tumor development [14]. However, with the advent of CAA tumor support, emphasis should be placed on the analysis of cellular lipid heterogeneity within the lipid bodies of the localized cells of the breast tumor and adjacent normal tissues that comprise the complex breast tumor microenvironment. Ultimately, there is a great need for true single-cell analysis that retains spatial localization within tumor tissues to discover lipid biomarkers of emerging disease for early detection, and gain an understanding of cellular processes at the onset of tumor development.

High-throughput single-cell analysis techniques have been developed utilizing capillary electrophoresis, flow cytometry, microfluidics [15-17] and printed microarrays [18]. However, spatial information is lost as these methods separate groups of cells from culture or tissues down to single cells. Raman is a non-destructive technique capable of single-cell lipid analysis using ratios of single bonded carbons versus double bonded carbons to identify the degree of saturation of fatty acyl chains present in a cell, but not the lipids themselves [19]. Matrix assisted laser desorption/ionization mass spectrometry (MALDI MS)

ISSN: 1927-7210 / E-ISSN: 1927-7229/16

^{*}Address correspondence to this author at the Department of Chemistry, University of North Texas, 1155 Union Circle #305070, Denton, TX 76203-5017, USA; Tel: (940) 369-8423; Fax: (940) 369-8474; E-mail: gyerbeck@unt.edu

is routinely used for the imaging of lipids of intact tissues with the capability of single-cell spatial resolution, but is still disadvantaged by the lengthy sample preparation times and the use of matrix that may alter or disburse cellular chemistry across a sample during application [15, 20]. Utilizing a focused ion beam, secondary ion mass spectrometry (SIMS) achieves subcellular resolution but causes excessive fragmentation resulting in loss of parent lipid identification and makes interpretation of spectra difficult [15, 16]. Furthermore, SIMS also requires an involved sample preparation method to remove the cellular membrane to analyze intracellular metabolites [21]. Lastly, Single-probe mass spectrometry has been developed to analyze single-cells with an achieved spatial resolution of roughly 8µm, but with a probe size of 6µm ultimately lacks the ability to analyze subcellular structures and has been described as targeting only cytoplasmic metabolites [22, 23]. Furthermore, the targeting precision of the technique is limited by the X,Y,Z stage's translational movement 0.1µm [22].

One-Cell analysis is a method developed by our group as a solution to the problem of lost spatial information during single-cell analysis capable of elucidating subcellular structures and their unique heterogeneities [13, 24-27]. The One-Cell technique encompasses nanomanipulatation for the extraction of targeted subcellular components coupled to nanoelectrospray ionization mass spectrometry (NSI-MS) for lipid analysis. One-Cell analysis is capable of individual whole cell extraction as well the targeted extraction of individual organelles. Using modified nanomanipulator, One-Cell analysis is capable of subcellular spatial resolution with a step size of 100 nm in coarse mode and 10 nm in fine mode. The nanomanipulator is equipped with multiple positioners to perform nanoextraction using quartz rods, micropipettes, and metal coated nano-spray capillary emitters. The positioners can also be fitted with end effectors to perform micro gripping and low impedance electrical characterizations. Extraction solvents can be tuned for the optimal extraction of specific analytes removing the need for additional sample cleanup. Cell cultures and tissues remain viable after analysis because extractions are performed in ambient laboratory conditions under a microscope and allowing for adjacent cells to remain unaffected so that they may undergo further analysis at a later time. Once a cell or organelle is extracted into a capillary, the analytecontaining capillary is then transferred to a nanoelectrospray ionization source and analyzed by tandem

mass spectrometry. Peaks of interest are selected for further analysis and fragmented. Based on the resulting fragmented peaks along with the calculation of neutral losses, structural information of the peak can be identified. However, this technique is limited in its throughput as each extraction and analysis requires roughly 10 minutes to perform. Furthermore, due to the small extraction volume of 10µL, mass spectrometry analysis time is limited to two minutes. In lieu of this short analysis window, automated instrument methods have been developed to perform complete analysis of the analytes of interest. Phelps *et al.* provides a complete description of the apparatus and method in detail [26].

Previously this technique has been used to identify the organellar heterogeneity of TG from individual lipid bodies extracted from neighboring cells within plant seeds [24, 25], mammalian cell culture [13, 26, 27] and human breast cancer tissue from a single donor [26]. Phelps et al., through the use of One-Cell, identified a decrease in the 54-acyl carbon TG species of adipocytes extracted from the tumorous breast tissue compared to extracted adipocytes from adjacent normal tissue of that same patient. Interestingly, Guo et al. identified an increase in the free fatty acid (FFA) species 18:1 in cancerous breast tissue compared to normal tissue [28], and therefore, we hypothesize that the tumorous cells may be consuming 18:1 FA species rather than continuing to store the FA as a fatty acvl constituent of TG species in their respective lipid bodies as a cause for this change in TG distribution. The work presented here demonstrates the use of One-Cell analysis coupled to tandem MS for the determination of the fatty acid composition of TG in normal and diseased breast tissue lipid bodies to determine if the relative decrease of TG species is a result of altered fatty acid composition due to tumor progression.

2. MATERIALS

Solvents for extraction include Chromosolv® Plus for HPLC chloroform (Sigma Aldrich, St. Louis, MO), 98% ammonium acetate (NH $_4$ OAc) (Sigma Aldrich, St. Louis, MO), and Optima LC/MS methanol (Fisher Scientific, Fairlawn, NJ).

Snap-frozen infiltrative ductal carcinoma tumor and normal adjacent breast tissues from two female donors were purchased from Cureline Inc. (Cureline, West San Francisco, CA). These tissues were cut into slices with a thickness of 80 µm using a CM 1850 cryomicrotome

(Leica Microsystems, Buffalo Grove, IL) and placed on glass coverslips for extraction.

3. METHODS

3.1. Extraction

One-cell analysis extractions were performed using a nanomanipulator equipped with two probers (DCG Systems Inc., Fremont, CA) mounted to an AZ100 microscope (Nikon, Melville, NJ). One prober was fitted with a quartz rod pulled using a P-2000 CO2-laser micropipette puller (Sutter Instruments, Novato, CA) to ~ 8µm. The second prober was fitted with a 1µm $(\pm 0.2 \mu m)$ diameter Pd/Au-coated Econo12 PicoTipTM Emitter (New Objective, Woburn, MA) backfilled with 10 µL of extraction solvent, 1:1 MeOH:CHCl₃ plus 0.1% NH₄OAc. Individual adipocytes were optically identified using the microscope, Figure 1, and then extracted following the procedure described in detail by Phelps et al. [26]. After extraction the emitters were then transferred to a nano-electrospray source (Proxeon Biosystems, Odense, Denmark) for nanoelectrospray ionization mass spectrometry analysis on a Thermo LTQ XL mass spectrometer (Thermo, San Jose, CA).

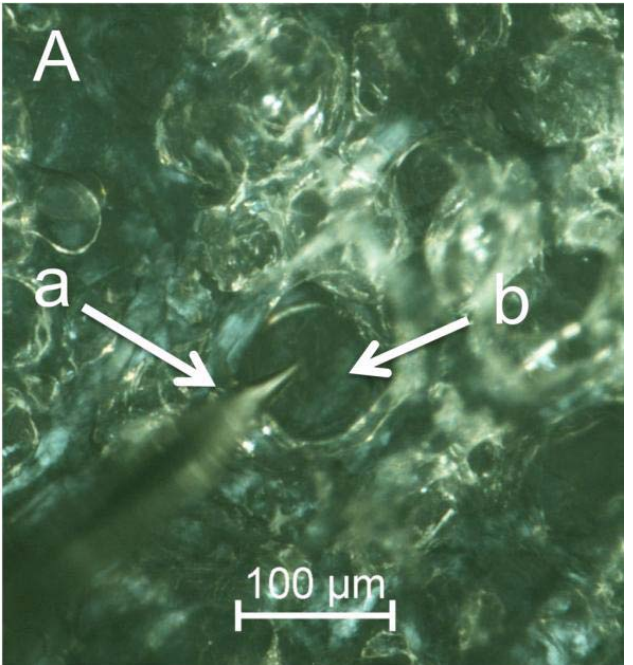
3.2. Mass Spectrometry Conditions

Triglyceride profiling experiments were analyzed in positive mode with a spray voltage of 1.8kV, a capillary inlet temperature of 225°C, with a mass range of m/z 700-1000. Fatty acid (FA) composition determination experiments were analyzed in positive mode with a spray voltage of 1.8kV, an inlet temperature of 225°C, a mass selection window of 1 Da, and a collision induced dissociation (CID) energy of 40%. FA determination mass spectra were collected through CID scans of the isolated peaks with masses corresponding to the 52:4, 52:3, 52:2, 52:1, 54:5, 54:4, 54:3, and 54:2 ammoniated TG species, respectively. FA species were identified as neutral losses due to the fragmentation of the TG ions, [M+NH₄]⁺, resulting in the diacylglycerol (DG) ion, [M+NH₄-(RCOOH+NH₃]⁺ as described by McAnoy et al. [29].

3.3 Data Analysis

3.1.1. TG Profile

Mass spectra data files were imported and plotted using the PSI-Plot software suite (Poly Software International, Pearl River, NY). The area under the curve was calculated for the individual areas for each of the regions corresponding to the 48-, 50-, 52-, 54, and 56-acyl carbon TG species using the <Calculate Area> function of the software suite. Finally, the ratio of the individual peaks to the total peak area were calculated and graphed to identify alterations in the TG profile as a function of the health state of the tissues.



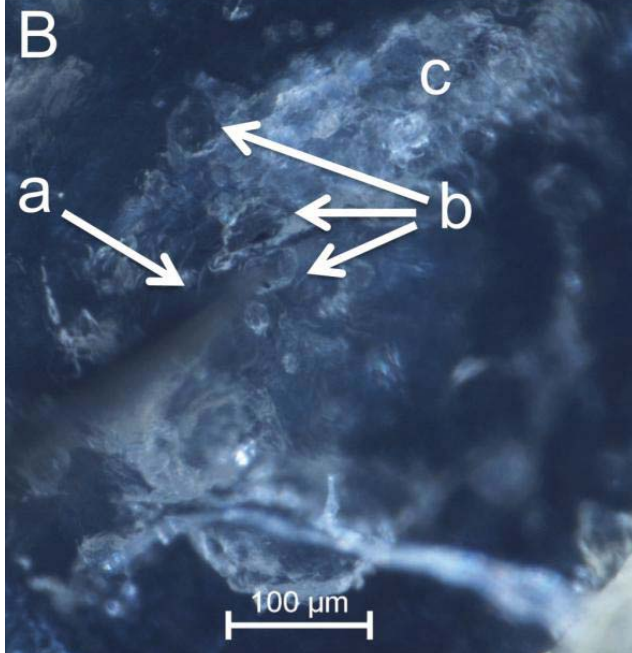


Figure 1: Bright field image of the nano-extraction of a single adipocyte from A) healthy breast tissue showing the emitter capillary tip (b) after entering the adipocyte (a); and B) cancerous tissue also showing the emitter tip (a) entering the adipocyte (b) surrounded by cancerous cells (c).

3.3.2. Fatty Acid Composition

The spectra for the CID scans corresponding to the masses of the 52:4, 52:3, 52:2, 52:1, 54:5, 54:4, 54:3, and 54:2 TG species were also imported and plotted using the PSI-plot software suite. The areas for all DG ion peaks were calculated. For each CID spectrum DG peak areas were then converted to relative abundance by dividing each individual DG ion peak area by the summed area of all DG ion peaks within the same CID spectrum.

4. RESULTS

One-cell analysis was performed on adjacent normal and tumor breast tissues from two female donors, each with infiltrative ductal carcinoma. Analysis consisted of nanomanipulation guided subcellular extraction of lipid droplets (LD) from a single adipocyte within a tissue sample. Analysis was performed in replicates of five to show reproducibility and that variations in signal were caused by sample heterogeneity and not by normal instrument variance.

4.1. Triglyceride Profiling

As ilustrated in Figure 2, the relative abundance averages of the TG peak areas of the normal extractions from the first tissue set were found to be 42.34%, 30.42%, 12.18%, 6.56%, and 5.33%; corresponding to the 52-, 54-, 56-, and 48-acyl carbon TG species. While the diseased tissue extractions relative abundance averages were 43.54%, 26.94%, 16.60%, 8.35%, and 4.56%; representing the 52-, 54-, 50-, 48, and 56-acyl carbon TG species. Within the second tissue set, the extractions from the normal tissue produced relative abundance averages of 42.81%, 26.43%, 16.51%, 7.81%, and 6.44%;

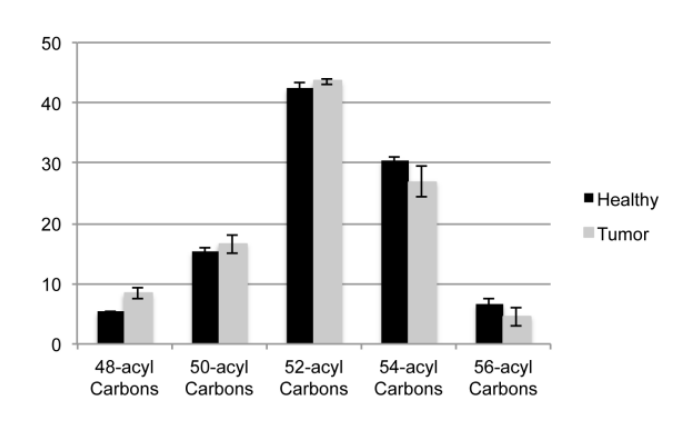
corresponding to the 52-, 54-, 50-, 56-, and 48-acyl carbon TG species. Lastly, the diseased tissue extractions had relative abundance averages of 42.71%, 20.05%, 15.67%, 5.84%, 4.35%, 1.67%, and 1.05%; corresponding to the 52-, 54-, 50-, 48-, and 56-acyl carbon species, respectively.

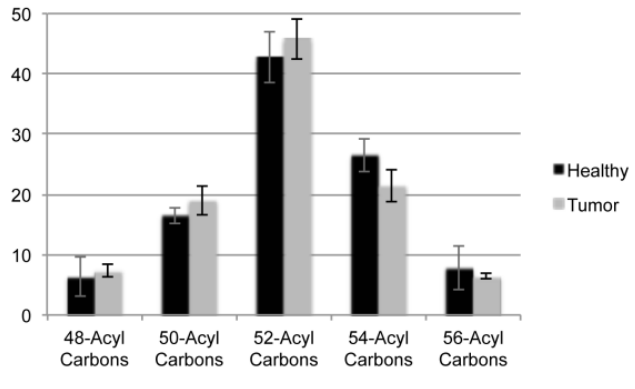
The ratio of the average relative abundance of the 52:54-acyl carbon TG species was calculated for all tissue extracts. The normal and diseased ratios were then compared for each tissue set. Ultimately, relative to the normal tissues there was a decrease of 9.98% and 14.98% in the abundance of the 54-acyl carbon species found in the diseased tissues of both tissue set 1 and 2, respectively. This decrease in the 54-acyl carbon species prompted further analysis of the tissues to determine if this change could be a result of disease related alterations in the fatty acyl constituents of the aforementioned TG species.

4.2. Fatty Acid Composition

Based on the results of the TG profiling data the largest change between the two health states of each tissue set was the decrease in the 54-acyl carbon TG species. To determine if this phenomenon was based on a change in fatty acid composition, a tandem MS/MS experiment was set up. The experiment was conducted in the same manor as the TG profiling experiment, with added CID analysis of the four most abundant individual TG species in each of the 52- and 54-acyl TG ranges.

Within the first set of tissues six FA species (16:0, 16:1, 18:0, 18:1, 18:2, and 20:1) were found to be present in all of the normal and diseased cells extracted from the first tissue set. These six fatty acids





В

Figure 2: Abundance of specific triglyceride (TG) species as a ratio of individual species peak area relative to the total TG area of **A**) tissue set 1 and **B**) tissue set 2, with standard deviation as the error bars.

Table 1: Relative Fatty Acid Composition of Cells Extracted from Tissue Set #1, Cells with a Gray Fill Indicate those Specific to all Tumor Cells Extracted

FA	Tumor Avg. Relative Abundance	Tumor Average Deviation	Healthy Avg. Relative Abundance	Healthy Average Deviation
16:0	1.04%	1.07%	0.00%	0.00%
16:1	2.05%	0.75%	1.84%	0.72%
17:1	0.14%	0.09%	0.00%	0.00%
18:0	11.18%	1.59%	11.29%	1.60%
18:1	47.70%	2.27%	48.74%	2.56%
18:2	16.68%	1.79%	17.03%	1.75%
18:3	0.88%	0.29%	0.00%	0.00%
20:0	0.14%	0.13%	0.00%	0.00%
20:1	0.56%	0.21%	0.58%	0.22%
20:2	0.30%	0.16%	0.00%	0.00%
20:3	0.17%	0.17%	0.00%	0.00%

account for 100% of the total FA composition of the normal extracted cells and 98.36% in the diseased cells. The remaining 1.64% in the diseased cells was made up of five FA that were unique to all extracted diseased tissue cells, 17:1, 18:3, 20:0, 20:2, and 20:3, Table 1.

Within the second tissue set, four FA species (16:0, 18:0, 18:1, and 18:2) were present in all of the normal and diseased cells extracted, and accounted for 98.24% and 88.64% of the total FA compositions, respectively. The remaining 1.76% of the normal FA composition is made up of 16:1 species, a FA that is absent from the diseased tissue cells extracted. Meanwhile, the remaining 11.36% is comprised of eight FA species (12:0, 17:1, 20:1, 20:2, 20:4, 22:3, 23:0, 26:0) present in all of the diseased tissue cells extracted and not in any of the normal tissue cells extracted, Table 2.

Table 2: Relative Fatty Acid Composition of Cells Extracted from Tissue Set #2, Cells with a Gray Fill Indicate those Specific to all Tumor Cells Extracted

FA	Tumor Avg. Relative Abundance	Tumor Average Deviation	Healthy Avg. Relative Abundance	Healthy Average Deviation
12:0	1.04%	1.07%	0.00%	0.00%
16:0	16.47%	3.85%	20.30%	0.83%
16:1	0.00%	0.00%	1.76%	0.38%
17:2	1.96%	1.37%	0.00%	0.00%
18:0	9.72%	2.23%	10.98%	1.08%
18:1	49.96%	2.16%	47.23%	1.14%
18:2	12.49%	2.55%	19.73%	0.92%
20:1	2.72%	2.05%	0.00%	0.00%
20:2	0.99%	0.95%	0.00%	0.00%
20:4	1.27%	0.86%	0.00%	0.00%
22:3	1.19%	1.28%	0.00%	0.00%
23:0	1.24%	1.40%	0.00%	0.00%
26:0	0.94%	0.89%	0.00%	0.00%

5. DISCUSSION

During times of cellular proliferation all cells are known to undergo metabolic variation but normal cells are capable of retaining metabolic regulation, while tumor cells lose metabolic regulation due to mutations in their signaling pathways [30]. It is the loss of regulation that leads to aberrant metabolite production making metabolites, such as lipids, ideal biomarkers for disease detection.

Hilvo et al. conducted a total lipid profiling study using whole tissue extracts to compare changes in tumor and normal breast lipids in which only a few tumor samples were found to have a decrease in TG species relative to their normal tissue counterparts [31]. While we do not see a complete decrease in TG, our findings do show a decrease in the relative abundance 54-acyl carbon TG of extracted diseased cells relative to the normal cells, which is consistent with the previous findings of Phelps et al. [26].

We originally hypothesized that the change in 54acyl TG species abundance would be due to a cancer related consumption of 18:1 FA species. Rather unexpectedly, a set of unique FA species specific to the disease tissue cells were identified, and the 18:1 FA species remained the most abundant FA species in all cells extracted. Furthermore, there was no significant change in the degree of saturation of FA present in the TG species of the normal and diseased tissue cells, however, in a recent study by Guo et al. cancerous breast tissue was found to contain an increased abundance of monounsatured FFA and a decrease in polyunsaturated FFA species [28]. In a recent total FA analysis of similar tissues, Azordegan et al. extracted lipids from whole tissues representing breast tumor, interface, and adjacent normal tissues to find increases in 18:0 FA species in breast tumors, and decreased abundance of 18:1, 18:2, and 18:3 in the tumor tissues [32]. Whereas in this study, no significant difference in the abundance of 18:0 was found among the tissue types while we saw no significant change in 18:1 and 18:2 species among the two tissues. The FA species 18:3 was only identified in the tumor cells extracted from tissue set one in our study and were not found in any of the other tissue cells extracted.

Of the thirteen unique FA species associated only with the cells extracted from disease tissue (tissue set 1: [17:1, 18:3, 20:0, 20:2, 20:3] and tissue set 2: [12:0, 17:2, 20:1, 20:2, 20:4, 22:3, 23:0, 26:0]) only one, 20:2, is found in both tissue sets. The 18:3 FA species was reported to be found only in breast cancer tissues

during a whole tissue extraction comparison of liver, pancreas, and breast cancer tissues to their normal counterparts [33]. The FA species 20:4, may be arachidonic acid depending on the location of its double bonds, however, this was not determined and therefore no claim to its incidence in these cancer tissues can be made. The presence of odd chain fatty acids, 17:1 and 17:2, may be due to an increased peroxidation of lipids in breast cancer patients as reported by Gupta et al., [34] possibly through alpha oxidation [35]. The remaining FA species (20:0, 20:2, 20:3, 12:0, 20:1, 22:3, 23:0, and 26:0) have all been associated with serum fatty acids in previous cancer related studies [12, 36] and may in fact be related to individual diets of the individuals associated with the tissues samples analyzed. While the importance of these disease specific fatty acid species is currently unknown, their identifications as fatty acyl constituents of stored triglycerides within the lipid bodies of breast tumor cells would not be known without the use of One-Cell analysis.

6. CONCLUSION

Due to the complexity of the breast tumor microenvironment, One-cell analysis is an ideal method to extract and analyze the lipids of individual cells and organelles within the breast tumor microenvironment to identify lipids specific to tumor progression. While other methods such as, time-offlight secondary ion mass spectrometry (ToF-SIMS) and probe electrospray ionization mass spectrometry (PESI-MS) are capable of identifying tumor cells from normal cells in a mixture [21] and determining tumor borders in live mice [37, 38], respectively, neither is capable of elucidating organelle specific lipids. Furthermore, the use of One-Cell analysis leaves unextracted cells intact for future analysis in tissues, or future biochemical analysis within in culture. The current application was tuned for the extraction of triglycerides, but simply changing the extraction solvent and mass spectrometer settings will allow for the analysis of any metabolite of interest.

Future work would ideally be focused on the analysis of more tumor tissues to create a larger data set to discover a breast cancer lipid biomarker present in all breast tumors. One-Cell analysis also needs to be expanded to other lipid classes and metabolites. Ultimately, One-Cell analysis is an ideal technique for the detection of tumor cells during on-site analysis of minimally invasive needle biopsies at the time of collection.

Much work has gone into identifying the pathways involved in obesity related cancer progression such as those relating to adipokines, estrogen, insulin, and proinflammatory cytokines [39]. Obesity considered to be a state of chronic inflammation that elicits an immune response that is known to create a local environment that is beneficial for the proliferation of adipocytes [40]. However, this increase in proliferation often leaves many cells in the immature preadipocyte form. These preadipocytes responsible for an increased secretion of proinflammatory cytokines, some of which are responsible for the recruitment of immune cells and the promotion of angiogenesis [40]. Many forms of cancer thrive in the presence of adipose tissue [41, 42] and the ability to analyze tumor microenvironments one cell at a time could provide an insight as to how the aforementioned pathways and secreted cytokines affect cells at the forefront of a progressing tumor. The use of One-cell analysis to gather information pertaining to the intracellular changes resulting from obesity relatedcancer pathways would be an integral part in the development of multidisciplinary research teams focused on elucidating the mechanism(s) of obesityrelated cancer progression to identify new therapeutic targets and develop personalized treatment plans.

ACKNOWLEDGEMENTS

This work was supported by the CPRIT High-Impact Research Award (RFA R-13-HIHR-1).

REFERENCES

- American Cancer Society. Cancer Facts & Figures 2015. [1] Atlanta: American Cancer Society 2015. http://www.cancer.org/research/cancerfactsstatistics/cancerfa ctsfigures2015/
- Dirat B, Bochet L, Dabek M, et al. Cancer-associated [2] adipocytes exhibit an activated phenotype and contribute to breast cancer invasion. Cancer Res 2011; 71: 2455-65. http://dx.doi.org/10.1158/0008-5472.CAN-10-3323
- [3] Tan J, Buache E, Chenard M-P, Dali-Youcef N, Rio M-C. Adipocyte is a non-trivial, dynamic partner of breast cancer cells. Int J Dev Biol 2011; 55: 851-59. http://dx.doi.org/10.1387/iidb.113365it
- Zhang Y. Daguinag AC. Amaya-Manzanares F. et al. Stromal [4] progenitor cells from endogenous adipose tissue contribute to pericytes and adipocytes that populate the tumor microenvironment. Cancer Res 2012; 72(20): 5198-208. http://dx.doi.org/10.1158/0008-5472.CAN-12-0294
- Kwan HY, Chao X, Su T, et al. Dietary lipids and adipocytes: [5] potential therapeutic targets in cancers. J Nutr Biochem 2015: 26: 303-11. http://dx.doi.org/doi:10.1016/j.jnutbio.2014.11.001
- Chajes V, Niyongabo T, Lanson M, et al. Fatty-acid [6] composition of breast and iliac adipose tissue in breastcancer patients. Int J Cancer 1992; 50(3): 405-08. http://dx.doi.org/10.1002/ijc.2910500314

- Timovska Y, Pivnyuk V, Todor I, Anikusko N, Chekhun V. [7] The spectrum of blood serum lipids in patients with breast cancer without metabolic syndrome. Exp Oncol 2011: 33(3): 190-92. http://www.ncbi.nlm.nih.gov/pubmed/21956478
- Abdelsalam KEA, Hassan IK, Sadig IA. The role of [8] developing breast cancer in alteration of serum lipid profile. J Res Med Sci 2012; 17(6): 562-65. http://jrms.mui.ac.ir/index.php/jrms/article/view/8492
- Kapil U, Bhadoria AS, Sareen N, Singh P, Dwivedi SN. Total [9] cholesterol and triglyceride levels in patients with breast cancer. J Breast Cancer 2013; 16(1): 129-30. http://dx.doi.org/10.4048/jbc.2013.16.1.129
- Sonawane A, Robin P. Tracking lipid changes in blood to [10] predict onset of cancer. Int J Pharma Bio Sci 2014; 5(4): (B) 942-48. http://www.ijpbs.net/cms/php/upload/3706_pdf.pdf
- Mishra S. Lipid profile in breast cancer patients. Int J Pharma Med Res 2015; 3(1): 29-35. http://www.woarjournals.org/IJPMR/vol_issue.php?abc1=8
- Chajes V, Thiebaut ACM, Rotival M, et al. Association [12] between serum trans-monounsaturated fatty acids and breast cancer risk in the E3N-EPIC study. Am.J Epidemiol 2008; 167(11): 1312-20. http://dx.doi.org/10.1093/aje/kwn069
- Phelps MS, Verbeck GF. A lipidomics demonstration of the [13] importance of single cell analysis. Anal Methods 2015; 7: 3668-70. http://dx.doi.org/10.1039/c5ay00379b
- Bell KE, Sebastiano KMD, Vance V, et al. A comprehensive [14] metabolic evaluation reveals impaired glucose metabolism and dyslipidemia in breast cancer patients early in the disease trajectory. Clin Nutr 2014; 33: 550-57. http://dx.doi.org/10.1016/j.clnu.2013.08.001
- [15] Trouillon R, Passarelli MK, Wang J, Kurczy ME, Ewing AG. Chemical analysis of single cells. Anal Chem 2013; 85: 522
 - http://dx.doi.org/10.1021/ac303290s
- [16] Rubakhin SS, Lanni EJ, Sweedler JV. Progress toward single cell metabolomics. Curr Opin Biotechnol 2013; 24: 95-104. http://dx.doi.org/10.1016/j.copbio.2012.10.021
- Zenobi R. Single-cell metabolomics: analytical and biological [17] perspectives. Science 2013; 342(6163): 1201. http://dx.doi.org/10.1126/science.1243259
- Ellis SR. Ferris CJ. Gilmore KJ. et al. Direct lipid profiling of [18] single cells from inkjet printed microarrays. Anal Chem 2012; http://dx.doi.org/10.1021/ac302634u
- [19] Wu H, Volponi JV, Oliver AE, et al. In vivo lipidomics using single-cell Raman spectroscopy. Proc Natl Acad Sci USA 2011; 108(9): 3809-14. http://dx.doi.org/10.1073/pnas.1009043108
- Boggio KJ, Obasuyi E, Sugino K, et al. Recent advances in [20] single-cell MALDI mass spectrometry imaging and potential clinical impact. Expert Rev Proteomics 2011; 8(5): 591-604. http://dx.doi.org/10.1586/epr.11.53
- Robinson MA, Graham DJ, Morrish F, Hockenbery D, [21] Gamble LJ. Lipid analysis of eight human breast cancer cell lines with ToF-SIMS. Biointerphases 2016; 11: 02A303. http://dx.doi.org/10.1116/1.4929633
- Pan N, Rao W, Kothapalli NR, et al. The single-probe: a [22] minaturized multifunctional device for single cell mass spectrometry analysis. Anal Chem 2014; 86: 9376-80. http://dx.doi.org/10.1021/ac5029038
- Pan N, Rao W, Yang Z. Single-cell MS and high-spatial-[23] resolution MS imaging under ambient conditions using a novel sampling device. LC GC N Am 2015; 33(6). http://www.chromatographyonline.com/single-cell-ms-andhigh-spatial-resolution-ms-imaging-under-ambientconditions-using-novel-sampling

- [24] Horn PJ, Ledbetter NR, James CN, et al. Visualization of lipid droplet composition by direct organelle mass spectrometry. J Biol Chem 2011; 286(5): 3298-306. http://dx.doi.org/10.1074/jbc.M110.186353
- [25] Horn PJ, Chapman KD. Organellar Lipidomics. Plant Signal Behav 2011; 6(10): 1594-96. http://dx.doi.org/10.4161/psb.6.10.17133
- [26] Phelps M, Hamilton J, Verbeck GF. Nanomanipulation-coupld nanospray mass spectrometry as an approach for single cell analysis. Rev Sci Instrum 2014; 85: 124101. http://dx.doi.org/10.1063/1.4902322
- [27] Phelps MS, Sturtevant D, Chapman KD, Verbeck GF. Nanomanipulation-coupled matrix-assited laser desorption/ionization-direct organelle mass spectrometry: a technique for the detailed analysis of single organelles. J Am Soc Mass Spectrom 2016; 27: 187-93. http://dx.doi.org/10.1007/s13361-015-1232-9
- [28] Guo S, Wang Y, Zhou D, Li Z. Significantly increased monounsaturated lipids relative to polyunsaturated lipids in six types of cancer microenvironment are observed by mass spectrometry imaging. Sci Rep 2014; 4: 5959. http://dx.doi.org/10.1038/srep05959
- [29] McAnoy AM, Wu CC, Murphy RC. Direct qualitative analysis of triacylglycerols by electrospray mass spectrometry using a linear ion trap. J Am Soc Mass Spectrom 2005; 16: 1498-509. http://dx.doi.org/10.1016/j.jasms.2005.04.017
- [30] Chandel NS. Navigating Metabolism. Cold Spring Harbor, New York: Cold Spring Harbor Laboratory Press 2015.
- [31] Hilvo M, Denkert C, Lehtinen L, et al. Novel theranostic opportunities offered by characterization of altered membrance lipid metabolism in breast cancer progression. Cancer Res 2011; 71(9): 3236-45. http://dx.doi.org/10.1158/0008-5472.CAN-10-3894
- [32] Azordegan N, Fraser V, Le K, et al. Carcinogenesis alters fatty acid profile in breast tissue. Mol Cell Biochem 2013; 374: 223-32. http://dx.doi.org/10.1007/s11010-012-1523-4
- [33] Budhu A, Terunuma A, Zhang G, et al. Metabolic profiles are principally different between cancers of the liver, pancreas, and breast. Int J Biol Sci 2014; 10(9): 966-72. http://dx.doi.org/10.7150/ijbs.9810

- [34] Gupta RK, Patel AK, Kumari R, et al. Interactions between oxidative stress, lipid profile and antioxidants in breast cancer: a case control study. Asian Pac J Cancer Prev 2012; 13: 6295-98. http://dx.doi.org/10.7314/APJCP.2012.13.12.6295
- [35] Jenkins B, West JA, Koulman A. A review of odd-chain fatty acid metabolism and the told of pentadecanoi acid (C15:0) and heptadecanoic acid (C17:0) in health and disease. Molecules 2015; 20: 2425-44. http://dx.doi.org/10.3390/molecules20022425
- [36] Pala V, Krogh V, Muti P, et al. Erythrocyte membrane fatty acids and subsequent cancer: a prospective Italian study. J Natl Cancer Inst 2001; 93(14): 1088-95. http://dx.doi.org/10.1093/jnci/93.14.1088
- [37] Mandal MK, Yoshimura K, Chen LC, et al. Application of probes electrospray ionization mass spectrometry (PESI-MS) to clinical diagnosis: solvent effect on lipid analysis. J Am Soc Mass Spectrom 2012; 23: 2043-47. http://dx.doi.org/10.1007/s13361-012-0462-3
- [38] Yoshimura K, Mandal MK, Hara M, et al. Real-time diagnosis of chemically induced hepatocelluar carcinoma using a novel mass spectrometry-based technique. Anal Biochem 2013; 441: 32-37. http://dx.doi.org/10.1016/j.ab.2013.06.017
- [39] Khan S, Shukla S, Sinha S, Meeran SM. Role of adipokines and cytokines in obesity-associated breast cancer: therapeutic targets. Cytokine Growth Factor Rev 2013; 24: 503-13. http://dx.doi.org/10.1016/j.cytogfr.2013.10.001
- [40] Gilbert CA, Slingerland JM. Cytokines, obesity, and cancer: new insights on mechanisms linking obesity to cancer risk and progression. Annu Rev Med 2013; 64: 45-57. http://dx.doi.org/10.1146/annurev-med-121211-091527
- [41] Nieman KM, Romero IL, Houten BC, Lengyel E. Adipose tissue and adipocytes support tumorigenesis and metastasis. Biochim Biophys Acta 2013; 1831(10): 1533-41. http://dx.doi.org/10.1016/j.bbalip.2013.02.010
- [42] Roberts DL, Dive C, Renehan AG. Biological mechanisms linking obesity and cancer risk: new perspectives. Annu Rev Med 2010; 61: 301-16. http://dx.doi.org/10.1146/annurev.med.080708.082713

Received on 25-03-2016 Accepted on 21-04-2016 Published on 06-05-2016

http://dx.doi.org/10.6000/1927-7229.2016.05.02.1

© 2016 Hamilton and Verbeck; Licensee Lifescience Global.

This is an open access article licensed under the terms of the Creative Commons Attribution Non-Commercial License (http://creativecommons.org/licenses/by-nc/3.0/) which permits unrestricted, non-commercial use, distribution and reproduction in any medium, provided the work is properly cited.